

# Aliasing error of the $\exp(\beta\sqrt{1-z^2})$ kernel in the nonuniform fast Fourier transform

Alex Barnett\*

January 28, 2020

## Abstract

The most popular algorithm for the nonuniform fast Fourier transform (NUFFT) uses the dilation of a kernel  $\phi$  to spread (or interpolate) between given nonuniform points and a uniform upsampled grid, combined with an FFT and diagonal scaling (deconvolution) in frequency space. The high performance of the recent FINUFFT library is in part due to its use of a new “exponential of semicircle” kernel  $\phi(z) = e^{\beta\sqrt{1-z^2}}$ , for  $z \in [-1, 1]$ , zero otherwise, whose Fourier transform  $\hat{\phi}$  is unknown analytically. We place this kernel on a rigorous footing by proving an aliasing error estimate which bounds the error of the one-dimensional NUFFT of types 1 and 2 in exact arithmetic. Asymptotically in the kernel width measured in upsampled grid points, the error is shown to decrease with an exponential rate arbitrarily close to that of the popular Kaiser–Bessel kernel. This requires controlling a conditionally-convergent sum over the tails of  $\hat{\phi}$ , using steepest descent, other classical estimates on contour integrals, and a phased sinc sum. We also draw new connections between the above kernel, Kaiser–Bessel, and prolate spheroidal wavefunctions of order zero, which all appear to share an optimal exponential convergence rate.

## 1 Introduction and main result

The NUFFT computes exponential sums involving arbitrary off-grid source or target points, at speeds scaling like those of the FFT for regular grids. It has a wide range of applications, including magnetic resonance imaging [17, 10, 21], computed tomography [12], optical coherence tomography [36], synthetic aperture radar [1], spectral interpolation between grids [20, Sec. 6] [14], and electrostatics in molecular dynamics [24, 31]; for reviews see [20, 16, 3]. Given nonuniform points  $x_j$ ,  $j = 1, \dots, M$ , which may be taken to lie in  $[-\pi, \pi)$ , complex strengths  $c_j$ , and a bandwidth  $N \in 2\mathbb{N}$ , the 1D type 1 NUFFT computes the  $N$  outputs

$$f_k := \sum_{j=1}^M c_j e^{ikx_j}, \quad -N/2 \leq k < N/2. \quad (1)$$

The type 2 is the adjoint of this operation: it computes at arbitrary real targets  $x_j$  the  $N$ -term Fourier series with given coefficients  $f_k$ ,

$$c_j := \sum_{-N/2 \leq k < N/2} f_k e^{-ikx_j}, \quad j = 1, \dots, M. \quad (2)$$

---

\*Center for Computational Mathematics, Flatiron Institute, Simons Foundation, New York, NY, USA

The above naturally generalize to dimension  $d > 1$ , and there are related flavors of forward and inverse tasks that we will not address here [8, 20]. Naively the sums (1) or (2) require  $\mathcal{O}(NM)$  work ( $N$  being the total number of modes in cases with  $d > 1$ ); NUFFT algorithms approximate them to a user-specified relative tolerance  $\varepsilon$  with typically only  $\mathcal{O}(M(\log 1/\varepsilon)^d + N \log N)$  work.

The most popular algorithm (see, e.g., [10, 20, 3]) for the type 1, taking the 1D case, fixes a fine grid with nodes  $2\pi l/n$ , for  $l = 0, \dots, n-1$ , where  $n = \sigma N$ , and  $\sigma > 1$  is an upsampling parameter. The data is first spread to a vector  $\{b_l\}_{l=0}^{n-1}$  living on this grid via

$$b_l = \sum_{j=1}^M c_j \tilde{\psi}(2\pi l/n - x_j), \quad l = 0, \dots, n-1, \quad (3)$$

where  $\tilde{\psi}(x) := \sum_{m \in \mathbb{Z}} \psi(x - 2\pi m)$  is the periodization of a “scaled” (dilated) kernel  $\psi(x) := \phi(nx/\pi w)$ , where  $\phi$  is some “unscaled” kernel, meaning its support is  $[-1, 1]$ . Thus  $w \in \mathbb{N}$  is the scaled kernel width in fine grid points. The output approximations  $\tilde{f}_k \approx f_k$  to (1) are then

$$\tilde{f}_k = p_k \sum_{l=0}^{n-1} e^{2\pi i l k/n} b_l, \quad -N/2 \leq k < N/2, \quad (4)$$

which is computed via a size- $n$  FFT followed by truncation to the desired output indices. The total effort is thus  $\mathcal{O}(Mw + \sigma N \log N)$ , or  $\mathcal{O}(Mw^d + \sigma^d N \log N)$  for  $d > 1$ . The “deconvolution” factors  $p_k$  in (4) are designed to undo the kernel convolution in (3), thus are usually chosen as

$$p_k = \frac{2\pi}{n\hat{\psi}(k)} = \frac{2}{w\hat{\phi}(\pi w k/n)}, \quad -N/2 \leq k < N/2, \quad (5)$$

where  $\hat{\cdot}$  indicates the Fourier transform according to the definition  $\hat{\psi}(k) = \int_{-\infty}^{\infty} \psi(x) e^{ikx} dx$ . The type 2 performs the adjoints of the above steps in reverse order, to give approximations  $\tilde{c}_j \approx c_j$  to (2). The goal of this paper is, given  $\sigma$ ,  $w$ , and a particular kernel  $\phi(z)$ , to bound the output errors  $\tilde{f}_k - f_k$  or  $\tilde{c}_j - c_j$  of this algorithm in exact arithmetic. These errors are due to *aliasing*, that is, the size of  $\hat{\psi}(k)$  in the “tails”  $|k| \geq n - N/2$  relative to its size in the output band  $|k| \leq N/2$ .

In the earliest NUFFT algorithms with rigorous error analysis,  $\phi$  was a truncated Gaussian [8, 34] or B-spline [4], and exponential (geometric) convergence in  $w$  was shown, i.e. the error is  $\varepsilon = \mathcal{O}(e^{-c_\sigma w})$ . At the standard choice  $\sigma = 2$ , the rates  $c_\sigma$  for both of these kernels correspond to around  $0.5w$  digits of accuracy [16]. However, because of the spreading cost  $Mw^d$ , minimizing  $w$  for a given  $\sigma$  and  $\varepsilon$  is crucial. It was thus a (perhaps surprising) discovery of Logan and Kaiser [19, 15, 17] that the “Kaiser–Bessel” (KB) Fourier transform pair (plotted in green in Fig. (1))

$$\phi_{\text{KB},\beta}(z) := \begin{cases} \frac{I_0(\beta\sqrt{1-z^2})}{I_0(\beta)}, & |z| \leq 1 \\ 0, & \text{otherwise,} \end{cases} \quad \hat{\phi}_{\text{KB},\beta}(\xi) = \frac{2}{I_0(\beta)} \frac{\sinh \sqrt{\beta^2 - \xi^2}}{\sqrt{\beta^2 - \xi^2}}, \quad \xi \in \mathbb{R}, \quad (6)$$

where  $I_0$  is the modified Bessel function [27, (10.25.2)], has a much higher rate, achieving over  $0.9w$  digits of accuracy (for an optimal scaling of parameter  $\beta$  with  $w$ ) at  $\sigma = 2$ ; see (11). The rigorous analysis, due to Fourmont [11, 12], is subtle. This rate is the conjectured best possible (see Sec. 5), namely that of the *prolate spheroidal wavefunction* (PSWF) of order zero [33, 29], the latter being the minimizer of the tail mass  $\|\hat{\phi}\|_{L^2(\{|\xi| > \beta\})}$  over functions  $\phi$  with support  $[-1, 1]$ . Thus (and because

it is simpler to evaluate than the PSWF), KB is popular in NUFFT code libraries, either in “forward mode” (spreading with  $\phi_{\text{KB},\beta}$ ) [9, 35, 21], or “backward mode” (spreading with a truncated  $\hat{\phi}_{\text{KB},\beta}$ ) [20].

Recently the author and coworkers released a library [3] whose high speed is in part due to the use of a new “exponential of semicircle” (ES) kernel,

$$\phi_{\text{ES},\beta}(z) := \begin{cases} e^{\beta(\sqrt{1-z^2}-1)}, & |z| \leq 1, \\ 0, & \text{otherwise,} \end{cases} \quad (7)$$

being simpler than either KB or PSWF, yet empirically having the same optimal rate and very similar errors. The ES kernel has since been used to accelerate Spectral Ewald codes for periodic electrostatic sums [31]. Its Fourier transform  $\hat{\phi}_{\text{ES},\beta}(\xi)$  is not known analytically, yet is easily evaluated by quadrature [3, Sec. 3.1.1]. The above three kernels are compared in Fig. 1 for small and large  $\beta$  parameters.

The main goal of this paper is to prove the following aliasing error convergence theorem applying to (7), which places this simple kernel (and hence algorithms which use it [3, 31]) on a rigorous footing. The rate will depend on the fixed upsampling factor  $\sigma > 1$ . We also assume, as is usual with KB [10], a kernel parameter  $\beta$  proportional to  $w$ . Specifically,

$$\beta(\sigma, \gamma, w) := \gamma\pi w(1 - 1/2\sigma), \quad (8)$$

where  $\gamma$  is a “safety factor”. At  $\gamma = 1$ , the cutoff (see Fig. 1(c,f)) in  $\hat{\psi}_{\text{ES},\beta}$  would coincide with the lowest aliased frequency  $k = n - N/2$ , so in practice one sets  $\gamma < 1$  (see Remark 3). Our main result concerns the constant  $\varepsilon_\infty$  in the standard  $\ell^1$ - $\ell^\infty$  output error bounds

$$\max_{-N/2 \leq k < N/2} |\tilde{f}_k - f_k| \leq \varepsilon_\infty \|\mathbf{c}\|_1 \quad (\text{type 1}), \quad \max_{1 \leq j \leq M} |\tilde{c}_j - c_j| \leq \varepsilon_\infty \|\mathbf{f}\|_1 \quad (\text{type 2}), \quad (9)$$

where we use vector notation  $\mathbf{c} := \{c_j\}_{j=1}^M$  and  $\mathbf{f} := \{f_k\}_{k=-N/2}^{N/2-1}$ .

**Theorem 1.** *(stated without proof as [3, Thm. 7]). Fix the number of modes  $N \in \mathbb{N}$ , the upsampled grid size  $n > N$  (hence the upsampling factor  $\sigma = n/N > 1$ ), and the safety factor  $\gamma \in (0, 1)$ . Then the constant bounding the error (9) for the 1D type 1 and 2 NUFFT in exact arithmetic, using the ES kernel (7) with  $\beta = \beta(\sigma, \gamma, w)$  defined by (8), converges with respect to the kernel width  $w$  as*

$$\varepsilon_\infty = \mathcal{O}\left(\sqrt{w} e^{-\pi w \gamma \sqrt{1-1/\sigma-(\gamma^{-2}-1)/4\sigma^2}}\right), \quad w \rightarrow \infty. \quad (10)$$

The rest of this paper breaks its proof into three stages: Section 2 reviews the standard bound for  $\varepsilon_\infty$  involving a phased sum over the Fourier transform  $\hat{\psi}$  of a general scaled kernel. Section 3 uses contour deformation and steepest descent to derive  $\beta \rightarrow \infty$  asymptotics for  $\hat{\phi}_{\text{ES},\beta}$ , both below and above cutoff, then proves two technical lemmas on the decay of  $\hat{\phi}_{\text{ES},\beta}$ . Section 4 brings in two lemmas to handle phased sinc sums, then combines all of these ingredients to complete the proof.

We conclude the paper in Section 5 by drawing new connections—apparent in Fig. 1(b,e)—between the ES, KB, and PSWF kernels, and discussing their shared optimal rate.

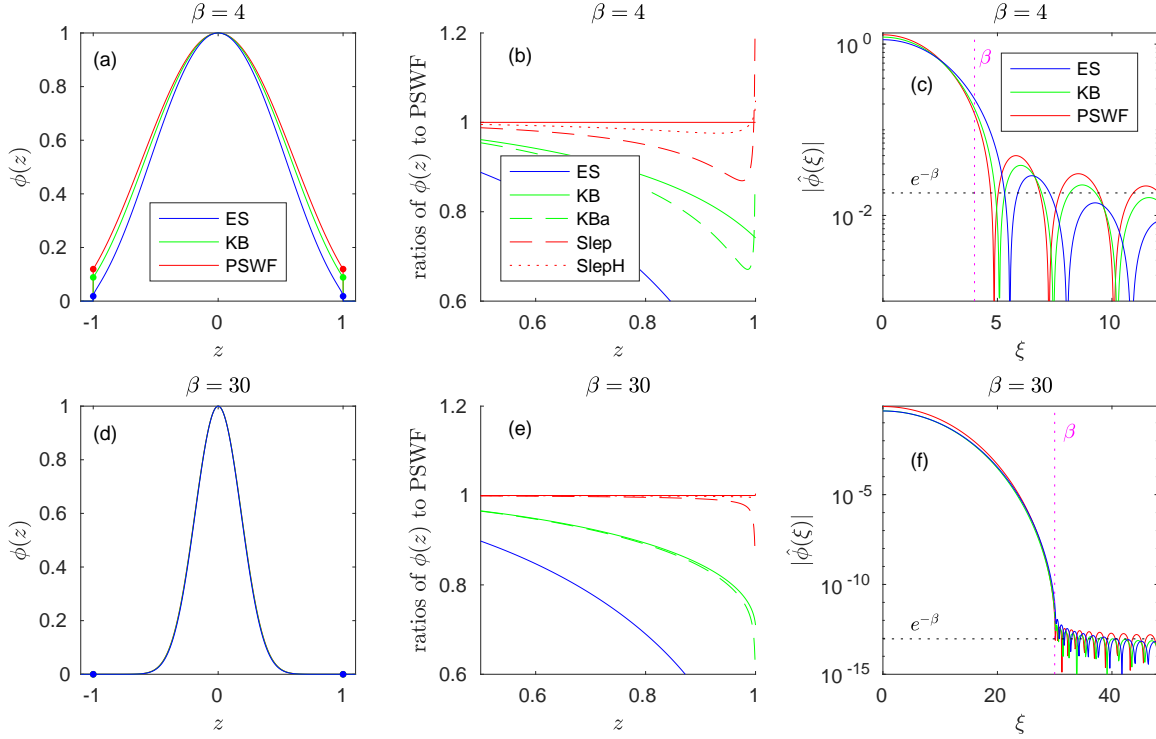


Figure 1: Comparison of the three unscaled spreading kernels  $\phi(z)$  on  $[-1, 1]$ : exponential of semi-circle (7) (ES, blue), Kaiser–Bessel (6) (KB, green), and the PSWF of order zero (blue; see Sec. 5). (a) The three kernels for parameter  $\beta = 4$ . Discontinuities at  $\pm 1$  are shown by dots. (b) Ratios to the PSWF, i.e.  $\phi(z)/\psi_0(z)$ , for: the other two kernels (solid lines), and asymptotic approximations “KBa” (37) (dashed green), “Slep” (Slepian’s upper form in (38), dashed red), and “SlepH” (a hybrid form (39), dotted red). (c) Magnitude of the three kernel Fourier transforms. All three have logarithm close to a quarter-ellipse below the cutoff frequency  $\xi = \beta$  (vertical dotted line), and are roughly bounded by  $e^{-\beta}$  (horizontal dotted line) above cutoff. The bottom row (d–f) shows the same as (a–c) but for  $\beta = 30$ . In (d) the three kernel graphs are indistinguishable.

**Remark 2** (Comparison to Kaiser–Bessel bounds). *In the limit  $\gamma \rightarrow 1^-$ , (10) approaches the exponential convergence rate of the rigorous estimate for the KB kernel [12] [20, App. C] when its parameter  $\beta$  is set by (8) with  $\gamma = 1$ ,*

$$\varepsilon_\infty \leq 4\pi(1 - 1/\sigma)^{1/4} \left( \sqrt{\frac{w-1}{2}} + \frac{w-1}{2} \right) e^{-\pi(w-1)\sqrt{1-1/\sigma}}. \quad (11)$$

*Unlike our result, this is a non-asymptotic bound with explicit constant, although we note that our algebraic prefactor is improved by a factor  $\sqrt{w}$ .*

**Remark 3** (Choice of safety factor  $\gamma$ ). *Taking  $\gamma \rightarrow 1^-$  maximizes the exponential rate in (10), but, in practice, choosing it slightly below 1 gives the smallest error: in [3] we recommend  $\gamma \approx 0.98$ ,*

similar to previous workers [17, Table II] [10, Fig. 11]. The restriction  $\gamma < 1$  in Thm. 1 is due to breakdown of the stationary phase estimate (20) at the cutoff frequency  $\xi = \beta$  where saddles head to  $\pm\infty$ . One may be able to extend the proof to  $\gamma = 1$  by using another method to bound  $\hat{\phi}$  near cutoff. However, because of the rapid growth in  $\hat{\phi}$  below cutoff (see, e.g., Fig. 1(e)), for any  $\gamma > 1$  the rate would necessarily be severely reduced.

**Remark 4** (Related work). A recent preprint by Potts–Tasche [30] claims to prove the same non-asymptotic exponential convergence rate on  $\varepsilon_\infty$ , but with explicit constant and tighter algebraic prefactor, for both the ES kernel and its variant  $\cosh \beta\sqrt{1-z^2}$  suggested in [3, Remark 13], but only for the parameter scaling  $\beta = 2w$ . While their discovery of explicit Chebychev expansions such as

$$\cosh \beta\sqrt{1-z^2} = I_0(\beta)T_0(z) + 2 \sum_{k=1}^{\infty} (-1)^k I_{2k}(\beta)T_{2k}(z), \quad \text{for } z \in [-1, 1]$$

is remarkable, the reliance on uncontrolled approximations that do not rigorously bound summations over  $k$  [30, pp. 17, 26, 34] we believe renders their claim heuristic. We also note that for low upsampling  $\sigma < 1/[2(1-2/\pi)] \approx 1.376$ , their choice  $\beta = 2w$  corresponds to  $\gamma > 1$ , so cannot give an optimal rate (see above Remark).

## 2 Aliasing error for type 1 and type 2 transforms

Here we recall a known rigorous estimate on the error of the 1D type 1 and 2 algorithms given in the introduction, performed in exact arithmetic. We start with the Poisson summation formula with an extra phase  $e^{i\theta}$ : for any  $\psi \in L^1(\mathbb{R})$  of bounded variation with Fourier transform  $\hat{\psi}$ , and any lattice spacing  $h > 0$ ,

$$\sum_{l \in \mathbb{Z}} e^{il\theta} \psi(x-lh) = \frac{1}{h} \sum_{m \in \mathbb{Z}} \hat{\psi}\left(-\frac{2\pi m + \theta}{h}\right) \exp\left(i\frac{2\pi m + \theta}{h}x\right). \quad (12)$$

The standard proof is that multiplication by  $e^{-ix\theta/h}$  makes the left-hand side a periodic function of  $x$ , hence its Fourier series coefficients are given by the Euler–Fourier formula. At any points  $x$  where the left-hand side is discontinuous, one must replace  $\psi(x-lh)$  by  $[\psi(x^+ - lh) + \psi(x^- - lh)]/2$  [2, §11.22].

We now derive the aliasing error for a general scaled kernel  $\psi(x)$ . For the type 1 NUFFT, setting  $h = 2\pi/n$ , inserting (3) into (4), and subtracting from the true answer (1) gives the error

$$\tilde{f}_k - f_k = \sum_{j=1}^M c_j \left[ p_k \sum_{l=0}^{n-1} e^{ihlk} \tilde{\psi}(lh - x_j) - e^{ikx_j} \right] =: \sum_{j=1}^M c_j g_k(x_j), \quad -N/2 \leq k < N/2. \quad (13)$$

Now writing the general ordinate as  $x$ , and applying Poisson summation (12) with  $\theta = hk$ ,

$$\begin{aligned} g_k(x) &:= p_k \sum_{l=0}^{n-1} e^{ihlk} \tilde{\psi}(lh - x) - e^{ikx} = p_k \sum_{l \in \mathbb{Z}} e^{ihlk} \psi(lh - x) - e^{ikx} \\ &= \frac{p_k}{h} \sum_{m \in \mathbb{Z}} \hat{\psi}(k + mn) e^{i(k+mn)x} - e^{ikx}. \end{aligned}$$

The choice (5) for  $p_k$  thus exactly kills the  $m = 0$  term, giving the well known aliasing error formula [34] [12, (4.1)] [10, Sec. V.B],

$$g_k(x) = \frac{1}{\hat{\psi}(k)} \sum_{m \neq 0} \hat{\psi}(k + mn) e^{i(k+mn)x} . \quad (14)$$

Thus, since  $|k| \leq N/2$ , error is controlled by a phased sum over the tails of  $\hat{\psi}$  at frequencies of magnitude at least  $n - N/2$ . Since type 2 is the adjoint of type 1 (or by similar manipulations to the above), its error is

$$\tilde{c}_j - c_j = \sum_{-N/2 \leq k < N/2} f_k \overline{g_k(x_j)} , \quad j = 1, \dots, M . \quad (15)$$

To summarize, let  $E$  be the “error matrix” with elements  $E_{kj} = g_k(x_j)$  given explicitly by (14) and  $E^*$  be its Hermitian adjoint, then the output aliasing error vectors are

$$\tilde{\mathbf{f}} - \mathbf{f} = E\mathbf{c} \quad (\text{type 1}), \quad \tilde{\mathbf{c}} - \mathbf{c} = E^*\mathbf{f} \quad (\text{type 2}). \quad (16)$$

From this the bounds (9) follow immediately if we define  $\varepsilon_\infty$  by a simple uniform bound on all matrix elements,

$$|E_{kj}| \leq \max_{|k| \leq N/2} \|g_k\|_\infty \leq \frac{\max_{|k| \leq N/2, x \in \mathbb{R}} \left| \sum_{m \neq 0} \hat{\psi}(k + mn) e^{i(k+mn)x} \right|}{\min_{|k| \leq N/2} |\hat{\psi}(k)|} =: \varepsilon_\infty . \quad (17)$$

Since the dynamic range over the output band,  $\hat{\psi}(0)/\hat{\psi}(N/2)$ , is not large [3, Remark 3], any lack of tightness in the second inequality in (17) is small.

**Remark 5.** *Users of NUFFT software often care about relative  $\ell^2$  errors, rather than absolute  $\ell^1$ - $\ell^\infty$  bounds such as (9). Making such bounds rigorous necessitates large prefactors in front of  $\varepsilon_\infty$ ; yet, in practice, relative  $\ell^2$  errors match  $\varepsilon_\infty$  quite well, for reasons discussed in [3, Sec. 4.2] [5, Sec. 4].*

### 3 Asymptotics of the Fourier transform of the ES kernel

Here we derive asymptotics in the width parameter  $\beta \rightarrow \infty$  of the Fourier transform of (7). From now on we abbreviate the kernel by  $\phi(z)$ , thus its Fourier transform by  $\hat{\phi}(\xi)$ . We introduce the scaled frequency

$$\rho := \xi/\beta . \quad (18)$$

The cutoff  $|\xi| = \beta$  (vertical line in Fig. 1(c,f)) is therefore at  $|\rho| = 1$ . The following shows that, up to weak algebraic prefactors: (a) below cutoff  $\hat{\phi}$  has a similar form to  $\phi$  itself, and that (b) above cutoff  $\hat{\phi}$  is oscillatory but uniformly exponentially small, with the same exponential rate  $e^{-\beta}$  as occurs for the KB and PSWF kernels (see Sec. 5).

**Theorem 6.** *Let  $\hat{\phi}$  be the Fourier transform of the ES kernel (7).*

(a) *Fix  $\rho \in (-1, 1)$ , i.e. below cutoff. Then,*

$$\hat{\phi}(\rho\beta) = \sqrt{\frac{2\pi}{\beta}} \frac{1}{(1-\rho^2)^{3/4}} e^{\beta(\sqrt{1-\rho^2}-1)} [1 + \mathcal{O}(\beta^{-1})] , \quad \beta \rightarrow \infty . \quad (19)$$

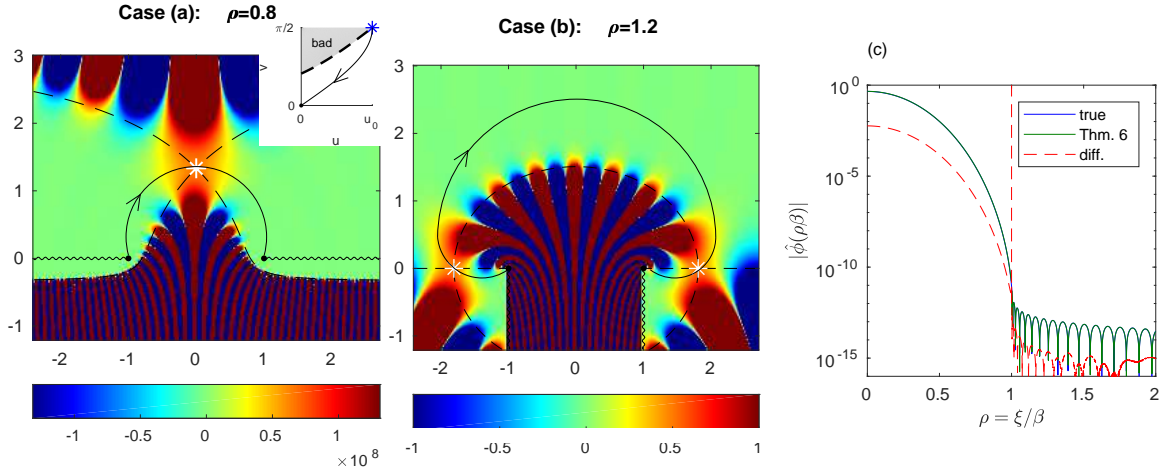


Figure 2: Real part of the integrand  $e^{\beta p(z)}$  appearing in the ES kernel Fourier transform (see (21)), plotted in the complex  $z$  plane, for  $\beta = 30$ . (a)  $\rho = 0.8$  (below cutoff). Also shown are the saddle point  $z_0$  (star), example contour (curve with arrow), boundaries where  $\text{Re } p(z) = \text{Re } p(z_0)$  (dashed lines), and standard branch cuts (wiggly lines). The inset shows the elliptic coordinate plane  $(u, v)$  for the right half of the  $z$ -plane, and the “bad” region where  $\text{Re } p(z) > \text{Re } p(z_0)$  (shaded). (b)  $\rho = 1.2$  (above cutoff); note change in color scale. The branch cuts of the square-root have been rotated to point downwards, exposing the two saddle points. (c) Comparison of the asymptotics (19) and (20) to the true  $\hat{\phi}$  (evaluated accurately by quadrature) for  $\beta = 30$ ; “diff.” shows their absolute difference. The weak algebraic divergence of (19)–(20) as  $\rho \rightarrow 1$  is highlighted by an asymptote.

(b) Fix  $\rho$ ,  $|\rho| > 1$ , i.e. above cutoff. Then,

$$\hat{\phi}(\rho\beta) = 2\sqrt{\frac{2\pi}{\beta}} e^{-\beta} \frac{\sin\left(\beta\sqrt{\rho^2-1} - \pi/4\right)}{(\rho^2-1)^{3/4}} [1 + \mathcal{O}(\beta^{-1})], \quad \beta \rightarrow \infty. \quad (20)$$

**Remark 7.** Fig. 2(c) shows the high accuracy of these asymptotic formulae (19)–(20) even at the modest value  $\beta = 30$ . Around two digits of relative accuracy are achieved everywhere shown except  $\rho \approx 1$ , where  $\hat{\phi}$  is already exponentially small. Remarkably, even details of the exponentially small tail oscillations at  $\rho > 1$  are matched to high relative accuracy. (However, Remark 9 will show that for  $\rho \gg 1$  relative error in this tail must diverge.)

*Proof.* In either case (a) or (b), the Fourier transform to be estimated is

$$\hat{\phi}(\rho\beta) = e^{-\beta} \int_{-1}^1 e^{\beta(\sqrt{1-z^2} + i\rho z)} dz = e^{-\beta} \int_{-1}^1 e^{\beta p(z)} dz, \quad p(z) := \sqrt{1-z^2} + i\rho z. \quad (21)$$

We apply saddle point integration in the complex  $z$  plane (see [26, Thm. 7.1, p. 127]; note that we have the opposite sign convention for  $p(z)$ ). This requires a smooth contour through an analytic region connecting  $-1$  to  $+1$ , avoiding branch cuts, passing through the saddle point(s), and along

which  $\operatorname{Re} p(z)$  has its global maximum at the saddle point  $z_0$  where  $p' = 0$ . The theorem then states that  $\int e^{\beta p(z)} dz = e^{\beta p(z_0)} \sqrt{\frac{2\pi}{-p''(z_0)\beta}} [1 + \mathcal{O}(\beta^{-1})]$ . Note that the standard branch cut  $(-\infty, 0)$  for the square-root gives cuts for  $p(z)$  at  $(-\infty, -1)$  and  $(1, +\infty)$ ; these cuts are shown in Fig. 2(a).

**Case (a).** We take  $0 \leq \rho < 1$ , since  $\hat{\phi}$  has even symmetry. Since  $\operatorname{Re} i\rho z$  becomes more negative as  $\operatorname{Im} z$  grows, the saddle  $z_0 = i\rho/\sqrt{1-\rho^2}$  is on the positive imaginary axis; see Fig. 2(a). To show the existence of a valid contour we switch to standard elliptical coordinates

$$z = \cosh(u + iv), \quad \operatorname{Re} z = \cosh u \cos v, \quad \operatorname{Im} z = \sinh u \sin v, \quad (22)$$

where  $\mu \geq 0$  and  $0 \leq v < 2\pi$  covers the plane. Since  $1 - z^2 = -\sinh^2(u + iv)$ , we get

$$\operatorname{Re} p(z) = \operatorname{Re} p(u, v) = (\cosh u - \rho \sinh u) \cdot \sin v, \quad (23)$$

which shows, remarkably, that the magnitude of the exponential in (21) is separable in this coordinate system. By solving  $p' = 0$  one finds that the saddle is at  $(u, v) = (\tanh^{-1} \rho, \pi/2)$ , where  $\operatorname{Re} p(z_0) = \sqrt{1 - \rho^2}$ .

Starting with the right half of the contour, we need to show that there is some smooth open path in  $(u, v)$  between  $(\tanh^{-1} \rho, \pi/2)$  and  $(0, 0)$  along which  $\operatorname{Re} p$  is everywhere less than  $\operatorname{Re} p(z_0)$ . At the endpoint,  $p = 0$ , which is indeed less than  $\operatorname{Re} p(z_0)$ ; yet it is possible that a barrier region of large  $\operatorname{Re} p$  prevents such a path from existing. We now show that no such barrier exists. The level curve  $\operatorname{Re} p(u, v) = \operatorname{Re} p(z_0)$  has positive slope in the  $(u, v)$  plane (see Fig. 2(a) inset). This is clear since the level curve intersects each line  $u = \text{constant}$  only once in  $(0, \pi/2)$ , because  $\sin v$  is monotonic there. Furthermore,  $\cosh u - \rho \sinh u$  is monotonically decreasing in  $[0, \tanh^{-1} \rho)$ , as is apparent from its derivative, so that the  $v$ -value of the intersection grows monotonically with  $u$ . This means that the “bad” region where  $\operatorname{Re} p(u, v) \geq \operatorname{Re} p(z_0)$  is confined to the upper left corner of the  $(u, v)$  rectangle (see inset), so there is no obstruction to crossing the diagonal while remaining small. The left half of the contour may then be chosen as a reflection of the right about the imaginary  $z$  axis. Thus a valid saddle contour exists.

At the saddle point,  $p''(z_0) = -(1 - \rho^2)^{3/2}$ , so that, taking the first term in the saddle point theorem [26, Thm. 7.1, p. 127] gives (19).

**Case (b).** Now  $\rho > 1$ . Solving  $p' = 0$  gives two saddle points on the real axis,  $z_0^{(\pm)} = \pm \rho/\sqrt{\rho^2 - 1}$ , where  $p(z_0^{(\pm)}) = 0$ . Since these lie on the standard branch cuts of the square-root, to make use of saddle point integration connecting  $z = -1$  to  $1$  in the upper half plane, one must *rotate the branch cuts downwards* to expose more of the Riemann sheet on which the contour lives. With this done, in order to avoid regions of large integrand, the contour must first head into the lower half-plane, pass up through  $z_0^{(-)}$ , into the upper half plane, down through  $z_0^{(+)}$ , and finish again from the lower half-plane; see Fig. 2(b). Both saddles contribute equally.

To show the existence of a valid contour we examine (23). The elliptical coordinates of the saddle points are  $(\coth^{-1} \rho, 0)$  and  $(\coth^{-1} \rho, \pi)$ . The factor  $\cosh u - \rho \sinh u$  vanishes on the ellipse  $u = \coth^{-1} \rho$  passing through the saddles, and, since it is monotonically decreasing, is positive for all smaller  $u$  and negative for all larger  $u$ . Thus  $\operatorname{Re} p < 0$  everywhere in the upper half plane outside the ellipse ( $u > \coth^{-1} \rho, 0 < v < \pi$ ), and in the lower half plane inside the ellipse with the slit  $[-1, 1]$  omitted ( $0 < u < \coth^{-1} \rho, \pi < v < 2\pi$ ). Thus a smooth contour exists passing through these regions via the two saddles.

To apply the theorem one must sum the left and right halves of the contour. However, on each half the theorem still cannot be used directly, since the start and end values  $\operatorname{Re} p(\pm 1) = 0$  are just



as large as the value at the saddles. Thus we remove fixed pieces of the contour around  $\pm 1$ , allowing the theorem to be applied. Using  $p(z_0^{(\pm)}) = \pm i\sqrt{\rho^2 - 1}$  at the two saddles,  $|p''(z_0^{(\pm)})| = (\rho^2 - 1)^{3/2}$ , the steepest descent directions  $e^{\mp i3\pi/4}$ , and summing the two contributions, gives (20).

Finally, we show that the contributions due to these fixed excluded pieces of the contour touching  $\pm 1$  are of lower order. Consider an excluded piece of contour in the lower half-plane from 1 to  $1 + b$ , where  $b \in \mathbb{C}$ ,  $\text{Im } b < 0$ , and  $1 + b$  is strictly inside the ellipse described above. We have already explained that  $p < 0$  on this contour, apart from at  $p(1) = 0$ . Writing  $z = 1 + t$ , and using  $p(1 + t) = i\rho + \sqrt{-2t - t^2} + i\rho t$ , The contour integral is

$$\int_0^b e^{\beta p(1+t)} dt = e^{i\rho} \int_0^b e^{\beta P(t)} dt, \quad \text{where } P(t) = -1\sqrt{2t + t^2} + i\rho t \sim -i\sqrt{2t} \text{ for } t \rightarrow 0.$$

All the conditions for Laplace's method for contour integrals [26, Thm. 6.1, p. 125] are met, with power  $\mu = 1/2$ , so its contribution is  $\sim -e^{i\rho}/\beta^2 = \mathcal{O}(\beta^{-2})$ , which is  $\beta^{3/2}$  times smaller than the contribution from the saddles. The same argument applies near  $-1$ . Thus these end contributions are of lower order and can be ignored in (20).  $\square$

**Remark 8.** *Informally Theorem 6 states: “the Fourier transform of the exponential of a semicircle is asymptotically the exponential of a semicircle, plus exponentially small tails.” This may be less of a surprise when it is recalled that the ES kernel is close to the PSWF (see Sec. 5), and that this “self-Fourier-transform” property holds exactly for the PSWF after truncation [33, 29].*

**Remark 9.** *It is tempting to fix  $\beta$  and interpret (20) as a decay  $\mathcal{O}(|\rho|^{-3/2})$ , i.e.  $\mathcal{O}(|\xi|^{-3/2})$ , which would be directly summable when inserted into (17). However, this is false. The kernel has discontinuities at  $z = \pm 1$  of strength  $e^{-\beta}$ , and is otherwise smooth, so the asymptotic must in fact be (at fixed  $\beta$ ),*

$$\hat{\phi}(\xi) \sim 2e^{-\beta} \frac{\sin \xi}{\xi} = \mathcal{O}(|\xi|^{-1}), \quad |\xi| \rightarrow \infty, \quad (24)$$

which is not absolutely convergent. This is an order-of-limits problem: (20) cannot be applied at fixed  $\beta$  in the limit  $|\rho| \rightarrow \infty$ , since the implied constant in the error term is unknown and must in fact be unbounded as  $|\rho| \rightarrow \infty$ . These growing saddle-point error terms are associated with the saddles  $z_0^{(\pm)}$  approaching the square-root singularity endpoints  $\pm 1$ . Empirically we find that the smooth transition from (20) to (24) occurs around  $\xi \approx \beta^2$ .

Because of the above remark, in order to get a rigorous error estimate we will also need the following, which bounds the  $\beta$ -dependence of the deviation (denoted by  $\hat{D}$ ) from the sinc function (24), uniformly in  $\beta$  and for sufficiently high frequencies  $\xi$ . To avoid ambiguities involving asymptotics with two parameters (here  $\beta$  and  $\xi$ ), for the rest of the section we avoid “big- $\mathcal{O}$ ” notation.

**Lemma 10.** *There exists a constant  $C > 0$ , independent of the shape parameter  $\beta$  and frequency  $\xi$ , such that for all  $\beta \geq 2$  and  $|\xi| \geq \beta^4$ , the Fourier transform of the ES kernel (7) is*

$$\hat{\phi}(\xi) = e^{-\beta} \left[ 2 \frac{\sin \xi}{\xi} + \hat{D}(\beta, \xi) \right], \quad \text{where } |\hat{D}(\beta, \xi)| \leq C \frac{\beta}{|\xi|^{5/4}}. \quad (25)$$

*Proof.* Since  $\hat{\phi}$  is symmetric, take  $\xi > 0$ . Since the top-hat function with value  $e^{-\beta}$  in  $[-1, 1]$ , and zero elsewhere, has the Fourier transform  $2e^{-\beta} \sin \xi/\xi$ , subtracting this top-hat from the kernel (7) leaves the Fourier transform deviation

$$\hat{D}(\beta, \xi) = \int_{-1}^1 (e^{\beta\sqrt{1-z^2}} - 1)e^{i\xi z} dz .$$

We deform this contour integral then apply Laplace-type estimates. Our deformed contour comprises three straight segments connecting the start point  $-1$  to  $-1+i$ , from there to  $1+i$ , and from there to the endpoint  $1$ . We write their contributions as  $\hat{D}(\beta, \xi) = I_1 + I_2 + I_3$ . Since at all points  $z$  on the middle segment we have  $|e^{i\xi z}| \leq e^{-\xi}$ , and  $|e^{\beta\sqrt{1-z^2}+i\xi z}| \leq e^{\sqrt{3}\beta-\xi}$ , but  $\xi \geq \beta^4$ , then  $I_2$  is exponentially small as  $\xi \rightarrow \infty$ , and can be dropped.

The first segment we parametrize by  $z = -1 + it$ , then split the integral to give

$$\begin{aligned} I_1 &= ie^{-i\xi} \int_0^1 (e^{\beta\sqrt{2it+t^2}} - 1)e^{-\xi t} dt \\ &= ie^{-i\xi} \left[ \int_0^{\xi^{-1/2}} (e^{\beta\sqrt{t}\sqrt{2i+t}} - 1)e^{-\xi t} dt + \int_{\xi^{-1/2}}^1 (e^{\beta\sqrt{t}\sqrt{2i+t}} - 1)e^{-\xi t} dt \right] . \end{aligned}$$

Since

$$|\sqrt{2i+t}| \leq 5^{1/4} \quad \text{for } 0 \leq t \leq 1 , \quad (26)$$

the lower integral is bounded in magnitude by

$$\left( \max_{0 \leq t \leq \xi^{-1/2}} e^{5^{1/4}\beta\sqrt{t}} - 1 \right) \cdot \int_0^{\xi^{-1/2}} e^{-\xi t} dt . \quad (27)$$

Here since  $\sqrt{t} \leq \xi^{-1/4} \leq 1/\beta$  we see that the first exponent is uniformly bounded by a constant, and using  $e^x - 1 \leq e^c x$  for  $x \leq c$ , we have that the first term in (27) is bounded by  $C\beta/\xi^{1/4}$ . The integral in (27) is bounded by  $1/\xi$ . Thus the lower integral is bounded by  $C\beta/\xi^{5/4}$ .

Turning to the upper integral in  $I_1$ , we bound its two additive terms separately,

$$\int_{\xi^{-1/2}}^1 e^{-\xi t} dt \leq \frac{e^{-\sqrt{\xi}}}{\xi} , \quad \text{and} \quad \int_{\xi^{-1/2}}^1 e^{\beta\sqrt{t}|\sqrt{2i+t}|-\xi t} dt \leq \int_{\xi^{-1/2}}^1 e^{-\xi t/2} dt \leq \frac{2e^{-\sqrt{\xi}/2}}{\xi} ,$$

which are both exponentially smaller than the lower integral, so can be dropped, giving  $|I_1| \leq C\beta/\xi^{5/4}$ . Here the second integrand was bounded for all  $t \geq \xi^{-1/2}$  using (26) and that  $2(5^{1/4})\beta \leq \xi^{3/4}$ , which, since  $\xi \geq \beta^4$ , holds as long as  $\beta^2 \geq 2(5^{1/4})$ , which is satisfied if  $\beta \geq 2$ .

The integrand on the third segment is the complex conjugate of the first, so  $I_3 = I_1^*$  and  $|I_3| = |I_1|$ . This proves (25).  $\square$

The above lemma excludes  $|\xi| < \beta^4$ , thus omits a growing (in  $\beta$ ) number of terms in the sum (17), so, for the reason given in Remark 9, one cannot use the saddle asymptotic (20) to cover these terms. This motivates the following intermediate estimate which allows smaller frequencies, has explicit  $\xi$  and  $\beta$  dependence, but (because of its second term) fails to be summable in  $\xi$ .

**Lemma 11.** For all  $\beta > 0$  and all  $|\xi| \geq 3\beta$ , the Fourier transform of the ES kernel (7) obeys

$$|\hat{\phi}(\xi)| \leq 9e^{-\beta} \left( \frac{\beta^2}{\xi^2} + \frac{1}{|\xi|} \right). \quad (28)$$

*Proof.* Bringing out the constant factor in the Fourier transform of (7), we wish to bound

$$e^{\beta} \hat{\phi}(\xi) = \int_{-1}^1 e^{\beta\sqrt{1-z^2} + i\xi z} dz.$$

Fixing  $\beta$  and  $\xi \geq 3\beta$ , we (again) deform the contour into the upper half plane, break it into three pieces, and estimate each piece. We will judiciously choose a radius

$$R = R_{\beta, \xi} = \sqrt{1 + [(\xi/2\beta)^2 - 1]^{-1}}, \quad \text{or} \quad (1 - R^{-2})^{-1/2} = \xi/2\beta. \quad (29)$$

Since  $(\xi/2\beta)^2 \geq 9/4$ , then  $1 < R \leq 3/\sqrt{5}$ . Let  $I_1$  be the integral along the real axis from  $-1$  to  $-R$ , let  $I_2$  be the integral along the semicircle  $|z| = R$ ,  $\text{Im } z \geq 0$ , and let  $I_3$  be the integral along the real axis from  $R$  to  $1$ . Then  $e^{\beta} \hat{\phi}(\xi) = I_1 + I_2 + I_3$ . Here the branch cuts of the integrand may be taken to lie below the real axis.

For all real  $z$  the integrand has unit magnitude, giving the trivial bound  $|I_1 + I_3| \leq 2(R - 1) \leq R^2 - 1$ . Using (29) and  $(\xi/2\beta)^2 \geq 9/4$  we see that this is bounded by  $(36/5)(\beta/\xi)^2 < 9(\beta/\xi)^2$ , giving the first term in (28).

On the upper semicircle we can limit the vertical exponential growth rate of  $e^{\beta\sqrt{1-z^2}}$  via

$$\text{Re } \sqrt{1-z^2} \leq (1 - R^{-2})^{-1/2} \text{Im } z, \quad \text{for all } z \text{ with } |z| = R \text{ and } \text{Im } z \geq 0. \quad (30)$$

This is proven by setting  $z = \sqrt{R^2 - b^2} + ib$  and  $\sqrt{1-z^2} = p + iq$ , so that  $\text{Re}(1-z^2) = p^2 - q^2 = 1 - R^2 - 2b^2$  and  $\text{Im}(1-z^2) = 2pq = -2b\sqrt{R^2 - b^2}$ . Eliminating  $q$  then solving the quadratic equation for  $p^2$  gives  $2p^2 = 1 - R^2 + 2b^2 + \sqrt{(R^2 - 1)^2 + 4b^2}$ . Applying the inequality  $\sqrt{A^2 + B^2} \leq A + B^2/2A$  for  $A > 0$  gives after simplification  $2p^2 \leq 2b^2/(1 - R^{-2})$ , which is equivalent to (30).

Applying (30) to  $I_2$ , the integrand magnitude obeys  $|e^{\beta\sqrt{1-z^2} + i\xi z}| \leq e^{[\beta(1-R^2)^{-1/2} - \xi] \text{Im } z} = e^{-(\xi/2) \text{Im } z}$ . This explains the choice (29): it limits the growth rate of  $e^{\beta\sqrt{1-z^2}}$  to at most half of the decay rate of  $e^{i\xi z}$ , so that decay wins. Now parametrizing the quarter-circle and using  $\sin \theta \geq 2\theta/\pi$  in  $0 \leq \theta \leq \pi/2$ , as in the proof of Jordan's lemma,

$$|I_2| \leq 2 \int_0^{\pi/2} e^{-(\xi/2)R \sin \theta} R d\theta \leq 2R \int_0^{\pi/2} e^{-(R\xi/\pi)\theta} d\theta \leq 2 \frac{3}{\sqrt{5}} \frac{\pi}{\xi} \leq \frac{9}{\xi},$$

giving the second term in (28). □

## 4 Phased sinc sums and proof of the main theorem

Firstly, to handle Fourier tails due to (exponentially small) discontinuities at the edge of the support of  $\phi$ , we need the following technical lemmas. The first lemma bounds a conditionally convergent sinc sum, but needs the second lemma which uniformly bounds the difference between an exponential sum and a sinc function. Recall the definition  $\text{sinc } x := (\sin x)/x$  for  $x \neq 0$ , or 1 otherwise.

**Lemma 12** (phased sinc sum). *Fix  $n > 0$  and  $\sigma > 1$ . Then there is a constant  $C$  such that for all  $b \geq 1$ ,  $x \in \mathbb{R}$ ,  $|k| \leq n/2\sigma$ , and  $\alpha > 0$ ,*

$$\left| \sum_{|m|>b} \frac{\sin \alpha(mn+k)}{mn+k} e^{i(mn+k)x} \right| \leq C \frac{\log b}{n}. \quad (31)$$

*Proof.* We apply Poisson summation (12) with grid spacing  $h = 2\pi/n$  to the top-hat function  $s(x) = 1$  in  $|x| \leq \alpha$ , zero otherwise. Since  $\hat{s}(k) = 2\alpha \operatorname{sinc}(\alpha k)$ , it gives

$$h \sum'_{|x-lh| \leq \alpha} e^{ikh} = 2\alpha \sum_{m \in \mathbb{Z}} \operatorname{sinc}(\alpha(mn+k)) e^{i(mn+k)x}, \quad k, x \in \mathbb{R}, \alpha > 0,$$

where the prime on the sum indicates that any extremal terms where  $|x-lh| = \alpha$  are to be given half their weight. Subtracting the  $m = 0$  term from both sides gives

$$h \sum'_{|x-lh| \leq \alpha} e^{ikh} - 2\alpha \operatorname{sinc}(\alpha k) e^{ikx} = 2\alpha \sum_{m \neq 0} \operatorname{sinc}(\alpha(mn+k)) e^{i(mn+k)x}. \quad (32)$$

Following an idea of Fourmont [11, Lemma 2.5.4], we use a triangle inequality on (31),

$$\left| \sum_{|m|>b} \frac{\sin \alpha(mn+k)}{mn+k} e^{i(mn+k)x} \right| \leq \left| \sum_{m \neq 0} \frac{\sin \alpha(mn+k)}{mn+k} e^{i(mn+k)x} \right| + \left| \sum_{1 \leq |m| \leq b} \frac{\sin \alpha(mn+k)}{mn+k} e^{i(mn+k)x} \right|.$$

We bound the first term by applying Lemma 13 to the left-hand side of (32) to get  $C/n$ , where  $C$  is independent of  $\alpha$ ,  $x$ , and  $k$  in its allowed domain, and bound the second term via the harmonic sum  $|\sum_{m=1}^b (k \pm mn)^{-1}| \leq C(\log b)/n$ , which holds since  $|k| \leq n/2$ . The second term dominates.  $\square$

**Lemma 13.** *Let  $\sigma > 1$ ,  $n > 0$ , and  $h = 2\pi/n$ . Then there is a constant  $C$  such that*

$$\left| h \sum'_{|x-lh| \leq \alpha} e^{ikh} - 2\alpha \operatorname{sinc}(\alpha k) e^{ikx} \right| \leq Ch, \quad \text{for all } x \in \mathbb{R}, |k| \leq \frac{n}{2\sigma}, \alpha > 0. \quad (33)$$

*Proof.* Note that  $2\alpha \operatorname{sinc}(\alpha k) e^{ikx} = \int_{x-\alpha}^{x+\alpha} e^{iky} dy = e^{ik(x-\alpha)} \sum_{j=0}^{J-1} e^{ikhj} \int_0^h e^{iky} dy + e_1 h$ , where  $J$  is the integer nearest  $2\alpha/h = n\alpha/\pi$ , and  $e_1$  is an end correction with  $|e_1| \leq 1$ . Into this we will insert  $\int_0^h e^{iky} dy = (e^{ikh} - 1)/ik = h e^{ikh/2} \operatorname{sinc}(kh/2)$ . Note also that the sum in (33) is a quadrature rule with weights  $h$  and one node per interval  $[x-\alpha+hj, x-\alpha+h(j+1)]$ ,  $j = 0, \dots, J-1$ , up to  $\mathcal{O}(h)$  end corrections. Each node is offset from the left end of its interval by  $\delta = \min_{l \in \mathbb{Z}, lh \geq x-\alpha} lh - (x-\alpha)$ , thus  $\sum'_{|x-lh| \leq \alpha} e^{ikh} = e^{ik(x-\alpha)} \sum_{j=0}^{J-1} e^{ikhj} e^{ik\delta} + e_2$ , where  $e_2$  is another end correction,  $|e_2| \leq 1$ . Combining results so far,

$$h \sum'_{|x-lh| \leq \alpha} e^{ikh} - 2\alpha \operatorname{sinc}(\alpha k) e^{ikx} = h e^{ik(x-\alpha)} [e^{ik\delta} - e^{ikh/2} \operatorname{sinc}(kh/2)] \sum_{j=0}^{J-1} e^{ikhj} + (e_2 - e_1)h.$$

The geometric sum is exactly  $(1 - e^{iJkh}) / (1 - e^{ikh}) = e^{i(J-1)kh/2} \sin(Jkh/2) / \sin(kh/2)$ , so is bounded in size by  $C/|kh|$ , independently of  $J$ , since  $|\sin(\theta/2)| \geq |\theta|/C$  for  $|\theta| \leq \pi/2$ , with  $C = \pi/\sqrt{2}$ . But since  $\delta \in [0, h)$ , the factor in square brackets is bounded in size by  $C|kh|$  for some  $C$ , over the domain  $|kh| \leq \pi/2$ , cancelling the  $1/|kh|$  blow-up. Thus all terms are uniformly bounded by  $Ch$ .  $\square$

**Remark 14** (Interpretations of Lemma 13). *The above lemma may be interpreted as an error bound when applying a simple  $\mathcal{O}(h)$ -accurate equispaced quadrature rule to  $\int_{x-\alpha}^{x+\alpha} e^{iky} dy$ . Remarkably, oscillatory cancellation makes the implied error constant independent of the domain width  $2\alpha$ .*

*A second interpretation is that it generalizes the little-known fact that the Dirichlet kernel [2, Sec. 11.10]  $D_N(\theta) := \sum_{n=-N}^N e^{in\theta} = \sin((N + \frac{1}{2})\theta) / \sin(\theta/2)$  is uniformly close to its non-periodic analogue  $2(N + \frac{1}{2}) \operatorname{sinc}((N + \frac{1}{2})\theta)$ , throughout  $N \in \mathbb{N}$  and  $|\theta| \leq \pi/2$  (say). The simpler estimates needed for this proof are  $|\operatorname{sinc}((N + \frac{1}{2})\theta)| \leq 1/(N + \frac{1}{2})|\theta|$  and  $|\operatorname{sinc}(\theta/2) - 1| \leq C|\theta|$ .*

Finally, we combine Lemma 12 with all of the results in Sec. 3 to prove the main Theorem 1.

*Proof.* Since  $n$ ,  $\sigma$ , and  $\gamma$  are fixed, then  $w$  and  $\beta$  are proportional via (8). We wish to bound  $\varepsilon_\infty$ , defined by (17), as  $w \rightarrow \infty$ , or, equivalently, as  $\beta \rightarrow \infty$ . Defining  $\alpha := \pi w/n$  as the half-width of the scaled kernel, writing (17) in terms of the unscaled kernel (7) gives

$$\varepsilon_\infty = \frac{\max_{|k| \leq N/2, x \in \mathbb{R}} \left| \sum_{m \neq 0} \hat{\phi}(\alpha k + \pi w m) e^{i(k+mn)x} \right|}{\min_{|k| \leq N/2} |\hat{\phi}(\alpha k)|}, \quad (34)$$

We now denote  $e^\beta$  times the sum in the numerator by

$$G(k, x) := e^\beta \sum_{m \neq 0} \hat{\phi}(\xi_m) e^{i\xi_m x / \alpha}, \quad \text{where } \xi_m := \alpha k + \pi w m. \quad (35)$$

The main task will be to prove that

$$|G(k, x)| = \mathcal{O}(1), \quad \beta \rightarrow \infty, \quad \text{uniformly in } x \in \mathbb{R}, |k| \leq n/2\sigma, \quad (36)$$

which will imply that the numerator of (34) is  $\mathcal{O}(e^{-\beta})$ . We will split the sum (35) into three ranges of  $|m|$ , then discard the phase information  $e^{i\xi_m x / \alpha}$  in all but the tail, where it becomes crucial.

We start by defining the closest range contribution by

$$G_1(k, x) := e^\beta \sum_{m \neq 0, |\xi_m| < 3\beta} \hat{\phi}(\xi_m) e^{i\xi_m x / \alpha},$$

which, using (8), involves at most five terms, independent of  $\beta$ . Since  $\gamma < 1$ , each term has  $|\xi_m/\beta| > 1$  so is strictly above cutoff. Thus, applying the leading saddle point result (20), each term contributes magnitude  $\mathcal{O}(1/\sqrt{\beta})$ , so  $G_1(k, x) = \mathcal{O}(1/\sqrt{\beta})$ .

The intermediate range contribution we define by

$$G_2(k, x) := e^\beta \sum_{3\beta \leq |\xi_m| \leq \beta^4} \hat{\phi}(\xi_m) e^{i\xi_m x / \alpha},$$

which involves  $\mathcal{O}(\beta^3)$  terms. Applying Lemma 11 and using  $\xi_m \sim c\beta m$  where  $c$  is a constant,

$$|G_2(k, x)| \leq C\beta^2 \sum_{m \leq \beta^3} \frac{1}{\beta^2 m^2} + C \sum_{m \leq \beta^3} \frac{1}{\beta m} = \mathcal{O}(1) + \mathcal{O}\left(\frac{\log \beta}{\beta}\right) = \mathcal{O}(1).$$

The remaining tail contribution to (35) is

$$G_3(k, x) := e^\beta \sum_{|\xi_m| \geq \beta^4} \hat{\phi}(\xi_m) e^{i\xi_m x / \alpha}.$$

We apply Lemma 10 (again noting the cancellation of  $e^\beta$ ) and the triangle inequality to get,

$$|G_3(k, x)| \leq \left| \sum_{|\xi_m| \geq \beta^4} 2 \frac{\sin \xi_m}{\xi_m} e^{i\xi_m x / \alpha} \right| + C \sum_{|\xi_m| \geq \beta^4} \frac{\beta}{\beta^{5/4} m^{5/4}}.$$

For the first (conditionally convergent) sinc sum, we apply Lemma 12 with  $b = \beta^3$ , which bounds the term by  $\mathcal{O}((\log \beta)/n\alpha) = \mathcal{O}((\log \beta)/\beta)$ , uniformly over  $|k| \leq n/2\sigma$  and  $x \in \mathbb{R}$ . The second term is summable so is  $\mathcal{O}(\beta^{-1/4})$ . Thus  $|G_3(k, x)| = \mathcal{O}(\beta^{-1/4})$ . Since  $G = G_1 + G_2 + G_3$ , (36) is proved.

The only remaining task is a lower bound on the denominator in (34). We exploit Theorem 6 below cutoff, i.e. (19). The minimum occurs at the edge of the usable band,  $|k| = N/2 = n/2\sigma$ , i.e.  $|\xi| := \alpha n/2\sigma = \pi w/2\sigma$ , i.e. scaled frequency  $\rho_e := \pi w/2\sigma\beta = (\gamma(2\sigma - 1))^{-1}$  using (8). Then the below-cutoff asymptotic (19) implies an upper bound on the inverse of the denominator,

$$|\hat{\phi}(\pi w/2\sigma)|^{-1} = \mathcal{O}(\sqrt{\beta} e^\beta e^{-\beta \sqrt{1-\rho_e^2}}) = \mathcal{O}(\sqrt{\beta} e^\beta e^{-\pi w \sqrt{\gamma^2(1-1/\sigma) - (1-\gamma^2)/4\sigma^2}}),$$

after simplification. Inserting this as the denominator of (34), and recalling (35)–(36), the factor  $e^\beta$  is cancelled. Since  $w$  is proportional to  $\beta$ , this proves (10).  $\square$

## 5 Connections between optimal rate spreading kernels

Here we link the ES, KB, and PSWF kernels asymptotically, discuss their common exponential convergence rate, conjecture that it is optimal, and conclude with a question.

The first connection starts with the KB kernel and inserts the large-argument asymptotic  $I_0(y) \sim e^y / \sqrt{2\pi y}$  [27, (10.3.4)], to give, for any fixed  $0 < a < 1$ ,

$$\phi_{KB,\beta}(z) \sim \frac{e^{\beta(\sqrt{1-z^2}-1)}}{(1-z^2)^{1/4}}, \quad z \in [-a, a], \quad \text{uniformly as } \beta \rightarrow \infty, \quad (37)$$

which is the ES kernel (7) with an extra algebraic prefactor. Experimentally dropping this prefactor in fact led us to the ES kernel in [3]. The closeness of (37) to KB, and the persistent algebraic difference between each of them and ES, is shown by Fig. 1(b,e).

In turn, KB is connected to the PSWF of order zero,  $\psi_0$ . While it is frequently stated in signal processing literature that KB is a “good” approximation to the PSWF [19, 17] [28, Sec. 7.5.3], we cannot find any quantification of how close in a mathematical sense (even in, say, [29, 6, 7]). One definition [33, 29] of  $\psi_0$  is the function with support in  $[-1, 1]$  with minimal  $L^2$ -norm (energy) outside the frequency interval  $[-\beta, \beta]$ . (Note that the PSWF parameter, usually called  $c$ , is set at  $c = \beta$ .) Slepian [32, (1.4)] derived the large- $\beta$  asymptotics,

$$\psi_0(z) = \begin{cases} C \frac{e^{\beta\sqrt{1-z^2}}}{(1-z^2)^{1/4}} (1 + \sqrt{1-z^2})^{-1/2} (1 + \mathcal{O}(\beta^{-1})) , & \beta^{-1/2} \leq |z| \leq 1 - \beta^{-1} \\ CI_o(\beta\sqrt{1-z^2}) (1 + \mathcal{O}(\beta^{-1})) , & 1 - \beta^{-1} \leq |z| \leq 1 . \end{cases} \quad (38)$$

Thus for all  $|z| \geq \beta^{-1/2}$ , normalizing  $\psi_0(0) = 1$ , this matches the KB kernel asymptotic, apart from a factor

$$\sqrt{2}(1 + \sqrt{1 - z^2})^{-1/2}$$

whose range is only  $[1, \sqrt{2}]$ . This asymptotic ratio function between PSWF and KB we have not found in either signal processing or mathematics literature, and it helps explain heuristically the similar performance of the kernels. The inverse of their ratio is plotted in Fig. 1(b,e) (green dashed line). Curiously, we find empirically that the *hybrid* form (Fig. 1(b,e), red dotted line)

$$\psi_{\text{StepH}}(z) = CI_o(\beta\sqrt{1 - z^2})(1 + \sqrt{1 - z^2})^{-1/2} \quad (39)$$

is a much better approximation to  $\psi_0$  in  $[-1, 1]$  than (38), with relative error uniformly  $< 0.2/\beta$ .

Other asymptotics for the PSWF are known. Inside the central (“turning point”) region  $|z| = \mathcal{O}(\beta^{-1/2})$ , the PSWF tends to the Gaussian  $\psi_0(z) = Ce^{-\beta z^2/2} + \mathcal{O}(\beta^{-1})$ , which has a width differing by only 4% from that of the optimal truncated Gaussian (shown in [3, Fig. 1.1(a)]). However, this is less useful than the above forms because of the inferior convergence rate of the Gaussian discussed in the introduction. This Gaussian limit can be derived by expansion in Hermite functions [22, §3.25] [29, Sec. 8.6]. Finally, WKBJ large- $\beta$  asymptotics of the PSWF due to Dunster [6], Ogilvie [25, Sec. 4.4], and others, uniformly cover more of  $[-1, 1]$ , but involve changes of variable that obscure any connection to KB or ES.

We now compare the aliasing error convergence rates of the three kernels, which is most relevant in applications. Remark 2 stated that in the limit  $\gamma \rightarrow 1^-$  the rate of the ES kernel matches that of KB. This rate  $e^{-\pi w \sqrt{1-1/\sigma}}$  may be traced to the optimal  $\beta$  choice (8), to both kernels having Fourier tails of order  $e^{-\beta}$  times their values at zero frequency (see (36) and Fig. 1(f)), and to the exponential-of-semicircle form of  $\hat{\psi}$  in the output band  $|k| \leq N/2$  (see [12, Prop. 2] and [3, Fig. 3.1(b)]). Does this rate also hold for the PSWF? Since  $\psi_0$  is a normalized eigenfunction of the projection operator ( $Q_c$  in [29]) onto the frequency band  $[-\beta, \beta]$ , its eigenvalue  $\mu_0 \leq 1$  gives the squared mass  $2\pi \int_{|\xi| < \beta} |\hat{\psi}_0(\xi)|^2 d\xi$ , and the remaining mass is  $1 - \mu_0 = 2\pi \int_{|\xi| > \beta} |\hat{\psi}_0(\xi)|^2 d\xi$ . It was proven by Fuchs [13] that

$$1 - \mu_0 \sim 4\sqrt{\pi}\beta e^{-2\beta}, \quad \beta \rightarrow \infty, \quad (40)$$

which shows that the  $L^2$ -norm of  $\hat{\psi}_0$  outside of  $[-\beta, \beta]$  is exponentially small with rate  $e^{-\beta}$ , which is indeed the same rate as in the ES and KB error bounds. Yet the  $L^2$ -norm does not bound the sum appearing in (17), so a bound on  $\varepsilon_\infty$  for the PSWF remains, to the author’s knowledge, heuristic. However, it strongly suggests the following.

**Conjecture 15.** *Fix  $N$  and the upsampling factor  $\sigma > 1$ , with  $n = \sigma N$ . Then  $c_{\text{optim},\sigma} := \pi\sqrt{1 - 1/\sigma}$  is the supremum of all values  $c$  for which there exists a family of kernels  $\psi_w$  of support  $[-\pi w/n, \pi w/n]$  with aliasing error bound (17) obeying*

$$\varepsilon_\infty = \mathcal{O}(e^{-cw}), \quad \text{as } w \rightarrow \infty. \quad (41)$$

This is consistent with the fact that numerical kernel optimization has produced only minimal reduction in errors relative to known kernels [17, 10, 18] (unless special assumptions on the power spectrum  $f_k$  are made [23]). The fact that the three kernels share this optimal rate tells us that their differing algebraic factors are surprisingly irrelevant for frequency localization.

**Remark 16** (Fast look-up tables for any smooth kernel). *The ease of numerical evaluation of a kernel is often claimed to be decisive in its choice: this was used to justify the KB over the PSWF kernel [19, 15, 17, 12, 18], and the ES over the KB [3]. However, look-up tables of coefficients of piecewise high-order polynomial interpolants evaluated via Horner’s rule, and modern open-source compiler vectorization, as used in FINUFFT [3, Sec. 5.3], mean that any smooth kernel with optimal rate, including the PSWF, could currently be used efficiently without loss of accuracy. Yet, it is possible that future hardware will have relatively faster `exp` evaluations, again making the simplest such kernel, ES, preferable.*

We finish with an open-ended question: ignoring algebraic prefactors, do all kernels on  $[-1, 1]$  that share the optimal rate  $c_{\text{optim},\sigma}$  have the asymptotic exponential form  $e^{\beta\sqrt{1-z^2}}$ , and, if so, why?

## Acknowledgments

The author has benefited from discussions with Charlie Epstein, Jeremy Magland, Leslie Greengard, Ludvig af Klinteberg, and Mark Dunster, and thanks Roy Lederman for MATLAB codes for accurate PSWF evaluation. The Flatiron Institute is a division of the Simons Foundation.

## References

- [1] F. Andersson, R. Moses, and F. Natterer. Fast Fourier methods for synthetic aperture radar imaging. *IEEE Trans. Aerospace Elec. Sys.*, 48(1):215–229, 2012.
- [2] T. M. Apostol. *Mathematical Analysis*. Addison-Wesley, Reading, MA, 1974.
- [3] A. H. Barnett, J. F. Magland, and L. af Klinteberg. A parallel non-uniform fast Fourier transform library based on an “exponential of semicircle” kernel. *SIAM J. Sci. Comput.*, 41(5):C479–C504, 2019.
- [4] G. Beylkin. On the fast Fourier transform of functions with singularities. *Appl. Comput. Harmonic Anal.*, 2:363–383, 1995.
- [5] A. Böttcher and D. Potts. Probability against condition number and sampling of multivariate trigonometric random polynomials. *Electron. Trans. Numer. Anal.*, 26:178–189, 2007.
- [6] T. M. Dunster. Uniform asymptotic expansions for prolate spheroidal functions with large parameters. *SIAM J. Math. Anal.*, 17(6):1495–1524, 1986.
- [7] T. M. Dunster. Asymptotics of prolate spheroidal wave functions. *J. Class. Anal.*, 11(1):1–21, 2017.
- [8] A. Dutt and V. Rokhlin. Fast Fourier transforms for nonequispaced data. *SIAM J. Sci. Comput.*, 14:1369–1393, 1993.
- [9] J. Fessler. Michigan image reconstruction toolbox, 2016. Available at <https://web.eecs.umich.edu/~fessler/irt/fessler.tgz>.



- [10] J. Fessler and B. Sutton. Nonuniform fast Fourier transforms using min-max interpolation. *IEEE Trans. Signal Proc.*, 51(2):560–574, 2003.
- [11] K. Fourmont. *Schnelle Fourier-Transformation bei nichtäquidistanten Gittern und tomographische Anwendungen*. PhD thesis, Univ. Münster, 1999.
- [12] K. Fourmont. Non-equispaced fast Fourier transforms with applications to tomography. *J. Fourier Anal. Appl.*, 9(5):431–450, 2003.
- [13] W. H. J. Fuchs. On the eigenvalues of an integral equation arising in the theory of band-limited signals. *J. Math. Anal. Appl.*, 9:317–330, 1964.
- [14] Z. Gimbutas and S. Veerapaneni. A fast algorithm for spherical grid rotations and its application to singular quadrature. *SIAM J. Sci. Comput.*, 5(6):A2738–A2751, 2013.
- [15] A. Goldstein and J. Abbate. Oral history: James Kaiser. <http://ethw.org/Oral-History:JamesKaiser>, 1997. online; accessed 2017-04-15.
- [16] L. Greengard and J.-Y. Lee. Accelerating the nonuniform fast Fourier transform. *SIAM Review*, 46(3):443–454, 2004.
- [17] J. I. Jackson, C. H. Meyer, D. G. Nishimura, and A. Macovski. Selection of a convolution function for Fourier inversion using gridding. *IEEE Trans. Medical Imaging*, 10(3):473–478, 1991.
- [18] M. Jacob. Optimized least-square nonuniform fast Fourier transform. *IEEE Trans. Signal Process.*, 57(6):2165–2177, 2009.
- [19] J. Kaiser. Digital filters. In J. Kaiser and F. Kuo, editors, *System analysis by digital computer*, chapter 7, pages 218–285. Wiley, 1966.
- [20] J. Keiner, S. Kunis, and D. Potts. Using NFFT 3 — a software library for various nonequispaced fast Fourier transforms. *ACM Trans. Math. Software*, 36(4), 2009.
- [21] J.-M. Lin. Python non-uniform fast Fourier transform (PyNUFFT): An accelerated non-Cartesian MRI package on a heterogeneous platform (CPU/GPU). *J. Imaging*, 4(3):51, 2018.
- [22] J. Meixner and F. Schäfke. *Mathieusche Funktionen und Sphäroidfunktionen*. Springer, Berlin, 1954.
- [23] F. Nestler. Automated parameter tuning based on RMS errors for nonequispaced FFTs. *Adv. Comput. Math.*, 42:889–919, 2016.
- [24] F. Nestler, M. Pippig, and D. Potts. Fast Ewald summation based on NFFT with mixed periodicity. *J. Comput. Phys.*, 285:280–315, 2015.
- [25] K. Ogilvie. *Rigorous asymptotics for the Lamé, Mathieu and spheroidal wave equations with a large parameter*. PhD thesis, University of Edinburgh, 2016.
- [26] F. W. J. Olver. *Asymptotics and special functions*. Academic Press, New York, 1974.

- [27] F. W. J. Olver, D. W. Lozier, R. F. Boisvert, and C. W. Clark, editors. *NIST Handbook of Mathematical Functions*. Cambridge University Press, 2010. <http://dlmf.nist.gov>.
- [28] A. V. Oppenheim and R. W. Schaffer. *Discrete-time signal processing*. Pearson Higher Education, Inc., 3rd edition, 2010.
- [29] A. Osipov, V. Rokhlin, and H. Xiao. *Prolate Spheroidal Wave Functions of Order Zero: Mathematical Tools for Bandlimited Approximation*, volume 187 of *Applied Mathematical Sciences*. Springer, US, 2013.
- [30] D. Potts and M. Tasche. Uniform error estimates for the NFFT, 2019. [arxiv:1912.09746v1](https://arxiv.org/abs/1912.09746).
- [31] D. S. Shamshirgar and A.-K. Tornberg. Fast Ewald summation for electrostatic potentials with arbitrary periodicity, 2017. [arxiv:1712.04732](https://arxiv.org/abs/1712.04732).
- [32] D. Slepian. Some asymptotic expansions for prolate spheroidal wave functions. *Journal of Mathematics and Physics*, 44(1-4):99–140, 1965.
- [33] D. Slepian and H. O. Pollak. Prolate spheroidal wave functions, Fourier analysis and uncertainty, I. *Bell Syst. Tech. J.*, 40:43–64, 1961.
- [34] G. Steidl. A note on fast Fourier transforms for nonequispaced grids. *Adv. Comput. Math.*, 9:337–352, 1998.
- [35] M. Uecker and M. Lustig. BART toolbox for computational magnetic resonance imaging, 2016. DOI: 10.5281/zenodo.592960. Available at <https://mrirecon.github.io/bart/>.
- [36] K. Zhang and J. U. Kang. Graphics processing unit accelerated non-uniform fast Fourier transform for ultrahigh-speed, real-time Fourier-domain OCT. *Opt. Express*, 18(22):23472–87, 2010.